SPE 106250

A Method to Improve the Mass Balance in Streamline Methods

Vegard Kippe, SINTEF, **Håkon Hægland**, University of Bergen, and **Knut–Andreas Lie**, SINTEF

This paper was prepared for presentation at the 2007 SPE Reservoir Simulation Symposium held in Houston, Texas, U.S.A., 26–28 February 2007.

Abstract

During the last decades, streamline methods have emerged as highly efficient simulation tools that are well-suited for e.g., history matching and simulation of large and complex reservoir models. Streamline methods are based on a sequential solution procedure in which pressure and fluid velocities are computed by solving a pressure equation on a grid in physical space and the fluid transport is computed by solving 1-D transport problems along streamlines. The sequential Eulerian-Lagrangian procedure is the key to the high computational efficiency of streamline methods. On the other hand, it necessitates mapping of saturations (or fluid compositions) back and forth between the Eulerian pressure grid and the Lagrangian streamlines. Unfortunately, this introduces mass-balance errors that may accumulate in time and in turn yield significant errors in production curves.

Mass-balance errors might be reduced by considering higher-order mapping algorithms, or by increasing the number of streamlines. Since the computational speed scales linearly with the number of streamlines, it is clearly desirable to use as few streamlines as possible. Here we propose a modification of the standard mapping algorithm that: (i) improves the mass-conservation properties of the method and (ii) provides high-accuracy production curves using few streamlines.

Mass conservation is improved by changing quantities in the transport equation locally, and we show that these modifications do not significantly affect the global saturation errors as long as a sufficient number of streamlines is used. Moreover, we propose an adaptive strategy for ensuring adequate streamline coverage. The efficiency and accuracy of the modified streamline method is demonstrated for Model 2 from the Tenth SPE Comparative Solution Project. Highly accurate production curves (compared to reference solutions) are obtained in less than ten minutes using one processor on a standard (Intel Core 2 Duo) desktop computer.

Introduction

Streamline simulation has experienced increasing industry interest and rapid technology development in recent years and is now a very efficient alternative to traditional flow modelling by numerical methods such as finite differences or finite volumes. Modern streamline methods can be used to compute complex flow physics such as compressible three-phase models with full PVT, multicomponent models or dual-porosity models (Thiele et al., 1997; Crane et al., 2000; Di Donato and Blunt, 2004). Still, streamline simulation is most efficient for simplified physical models and engineering queries based on the 80-20 principle: 80% of the answer in 20% of the time available (Thiele, 2005). In particular, due to its low memory requirements and high computational efficiency, streamline simulation today offers the opportunity to solve outstanding engineering queries that might otherwise be difficult or impossible to address using other approaches.

Streamline simulators are particularly suitable for solving large and geologically complex models, where the fluid flow is dictated primarily by heterogeneities in rock properties (permeability, porosity and faults/fractures), well positions, and phase mobilities. The typical application is for production regimes involving fluid displacement, e.g., water flood or gas injection. Other mechanisms, like capillary effects and expansion-driven flows, may be modelled, but not with the same degree of accuracy and efficiency. Primary examples of application are flow simulations on multimillion geocellular models of complex heterogeneity, and repeated simulations on equiprobable geological realisations to quantify sensitivity of model parameters and uncertainties in prediction forecasts. Generally, streamline

simulators are progressively being used more by operating companies as an alternative to traditional reservoir simulators in several reservoir engineering workflows, including: screening of enhanced recovery projects, rapid sensitivity studies, history matching, uncertainty assessment, upscaling, flood optimization, or simulation studies of sector or full-field models.

The computational setup within a streamline simulator can be briefly described as follows. First, the pressure distribution over a conventional 3-D grid is computed in order to determine the trajectories of 1-D streamlines that represent flow-paths. Next, the material balance equations can be transformed in terms of the so-called time-of-flight along a streamline and split into two parts, namely the part along the streamline and the part in the direction of gravity. These 1-D equations are then solved by an appropriate numerical method and the resulting saturation or concentration values are mapped back onto the 3-D grid. In each time-step, the velocity field is recomputed, which implies that streamline trajectories will change in time for dynamic flow conditions. For a more in-depth description of streamline simulation and an overview of the literature in this field, we refer the reader to the upcoming textbook by Datta-Gupta and King (to appear) or to the survey papers by Thiele (2005) and King and Datta-Gupta (1998).

The underlying mathematical formulation is both the strength and the weakness of streamline simulation. The operator splitting and the Lagrangian spatial discretization, which are fundamental assumptions of streamline methods, are the keys to obtaining high efficiency:

- The operator splitting used to decouple the computation of the velocity field (i.e., pressure) and the fluid transport has the effect that the size of the pressure steps is dictated by the flow dynamics, and not by the spatial (finite-difference) discretization. For e.g., water flood problems, this usually means that velocity fields and streamlines only need to be updated infrequently.
- The 1-D transport problems along streamlines and gravity lines can be solved very efficiently such that the computational complexity of the transport step scales linearly with the number of streamlines and the number of cells traversed by each streamline.
- The number of streamlines typically required to obtain an acceptable accuracy increases linearly with the number of active cells.

These three points, together with the existence of near-linear complexity linear solvers for the pressure equation (Stüben, 2000), imply that streamline simulation scales (almost) linearly with model size, may be very memory efficient, and offers a natural potential for parallel implementation. However, it is also evident that streamline simulation will loose its high efficiency for flows with a very strong coupling between the pressure and the mass transport equation.

Similarly, it is clearly desirable to use as few streamlines as possible to ensure efficient flow simulation. On the other hand, the set of streamlines should be representative and sufficiently dense to ensure accurate prediction of flow patterns and production responses, and to limit errors in the mass balance. Lack of mass conservation is a problem of particular concern to reservoir engineers, and in this paper we will try to analyse the lack of mass conservation and suggest methodological improvements that will strongly improve the mass balance. This will in turn allow a significant reduction in the number of streamlines required to ensure highly accurate production curves.

The rest of the paper is organized as follows: In the next two sections we define our model problem and describe what we shall refer to as our "standard" or "original" streamline method. The mass-balance problems are then illustrated with an example, and we utilize a description of the streamline spatial discretization given by Jimenez et al. (2005) to explain the problem. We propose a change of the original streamline method, and demonstrate that the modified approach improves the mass balance and gives accurate production curves using very few streamlines for a large and complex reservoir model. We then study the performance for various flow conditions on a very simple model and propose a strategy for ensuring adequate streamline coverage, before demonstrating applicability to a history-matching problem with more than a million grid blocks and 69 producers. Some final remarks then concludes the paper.

Model Problem

Since our focus in this paper is on the mass-balance properties of streamline methods, we will consider a simplified model for water flooding. That is, we assume immiscible, incompressible two-phase flow and disregard gravity and capillary forces. Our flow model then consists of an elliptic pressure equation

$$\nabla \cdot \mathbf{u} = q_t, \qquad \mathbf{u} = -\lambda_t(S)\mathbf{K}\nabla p, \tag{1}$$

and quasilinear hyperbolic transport equation

$$\phi\frac{\partial S}{\partial t} + \nabla \cdot (f_w(S)\mathbf{u}) = q_w. \tag{2}$$

The primary unknowns in the coupled system (1)–(2) are the pressure p, the total (Darcy) velocity $\mathbf{u}$, and the water saturation S. The underlying porous rock formation is modelled in terms of the absolute permeability $\mathbf{K}$ and the porosity ϕ, which henceforth are assumed to depend on the spatial variable only. Finally, $\lambda_t = \lambda_w + \lambda_o$ denotes the total mobility, where the mobility of each phase, λ_j is given as the relative permeability k_{rj} of phase j divided by the phase viscosity μ_j $(j = o, w)$, and $f_w = \lambda_w/\lambda_t$ is the fractional flow of water.

The Streamline Method

The streamline method is based on a sequential solution procedure. First the known initial saturation distribution is used to compute the mobilities $\lambda_t(S)$ in (1), after which the pressure equation can be solved to give total velocity $\mathbf{u}$ and pressure distribution p. Next, the total velocity $\mathbf{u}$ is kept fixed in (2), while the saturation is advanced a given time step. The new saturation values are used to update the mobilities in (1), the pressure equation is solved again, and so on.

Instead of discretizing and solving (2) directly on a grid, a streamline method decouples the three-dimensional equation into multiple one-dimensional equations along streamlines by introducing the time-of-flight variable,

$$\tau(s) = \int_0^s \frac{\phi(\zeta)}{|\mathbf{u}(\zeta)|}\mathrm{d}\zeta, \tag{3}$$

which is the time it takes a passive particle to travel a distance s along a streamline. In differential form (3) becomes,

$$\frac{\partial \tau}{\partial s} = \frac{\phi}{|\mathbf{u}|} \quad \Longleftrightarrow \quad \mathbf{u}\cdot\nabla\tau = \phi. \tag{4}$$

Moreover, we have that $\partial/\partial\tau \equiv \mathbf{u}\cdot\nabla$, which combined with (4) can be used to rewrite the saturation equation (2) as a one-dimensional equation to be solved along each streamline,

$$\frac{\partial S}{\partial t} + \frac{\partial f_w}{\partial \tau} = 0. \tag{5}$$

The solution to the full three-dimensional problem (2) is obtained by tracing numerous streamlines in the domain, mapping the initial saturation distribution from the 3-D pressure grid to the one-dimensional streamlines, and then solving (5) along each streamline. Afterwards, the new saturation values along streamlines must be mapped (or averaged) back to the underlying 3-D grid to allow updating of the mobilities before the pressure equation can be solved to recompute the velocity field.

A Specific Implementation. An implementation of the streamline method can be characterized by (i) the procedure for tracing streamlines, (ii) the choice of one-dimensional solver, (iii) the strategy for spatial distribution of streamlines, and (iv) the algorithms for mapping solution values back and forth between streamlines and the underlying (pressure) grid. We now describe what we shall refer to as our "standard" or "original" streamline method.

In this work we only consider models with Cartesian geometry, and we therefore use a simple semi-analytical tracing procedure due to Pollock (1988). Given the entry point and constant normal velocities on faces of a grid-block, Pollock's algorithm computes the exit point and the incremental time-of-flight associated with transversing the grid-block by assuming linear velocity variation in each direction. This way, each streamline can be traced numerically on a block-by-block basis from injector to producer or vice versa, or alternatively from an arbitrary point in the reservoir and forward to the producer and backward to the injector. After the tracing, each streamline is given as the indices of the blocks the streamline traverses, the entry and exit points, and the incremental time-of-flights for each block. These increments form the blocks in the streamline grid $\{\Delta\tau_{sl,i}\}$ on which (5) will be solved.

To solve the one-dimensional problems we employ front-tracking (see, e.g., Holden and Risebro, 2002), which is also applied in a commercial streamline simulator (Bratvedt et al., 1993; Bradtvedt et al., 1994). The front-tracking method is unconditionally stable and can directly utilize the time-of-flight grid resulting from the streamline trace, which makes the method very efficient and devoid of numerical diffusion. In contrast, solvers based on a finite-volume formulation typically need to map the initial data to a more regular grid (Batycky, 1997; Thiele, 2005).

The initial values for the one-dimensional problems are obtained by picking up the piecewise constant values from the underlying (pressure) grid, i.e., the grid-to-streamline mapping is the simplest possible,

$$S_{sl,i} = S_i. \tag{6}$$

To map values from the streamlines back to the grid, we use volumetric averaging. Volumes are associated with streamlines by considering each streamline as the centreline, or more precisely, as a representation of the cross-section, of a streamtube with an associated constant volumetric flux $q_{sl} = \mathbf{u}(\zeta)A(\zeta)$. This gives the volume of the streamline as,

$$\begin{aligned} V_{sl} \equiv V_{st} &= \int_0^s \phi(\zeta)A(\zeta)\mathrm{d}\zeta \\ &= \int_0^s q_{sl}\frac{\phi(\zeta)}{\mathbf{u}(\zeta)}\mathrm{d}\zeta = q_{sl}\tau_{sl}. \end{aligned} \tag{7}$$

The volume of a streamline in grid-block i is then $V_{sl,i} = q_{sl}\Delta\tau_{sl,i}$, and the precise definition of the streamline-to-grid volumetric averaging is,

$$S_i = \frac{\sum_{sl} S_{sl,i}V_{sl,i}}{\sum_{sl} V_{sl,i}}. \tag{8}$$

We note that considering streamlines as fluid carriers also makes it natural to define production characteristics simply by summing the contributions from all streamlines connected to each well. For long time-steps, the fractional flow of water at a producer may vary significantly; hence we measure the accumulated production along each streamline and define the total water production during a time-step of size Δt by,

$$\mathrm{PRD}_{\Delta t} = \sum_{sl} q_{sl}\int_{\Delta t} f_{w,sl}(t)\ \mathrm{d}t. \tag{9}$$

The values of (8) and (9), and the accuracy with which these values approximate the true saturation values and production increments, depend on how fluxes are assigned to the streamlines/streamtubes, and this may again be related to the procedure for distributing streamlines in the reservoir. Here we generate equally spaced starting points on the faces of grid-blocks containing injection wells. The number of starting points on each face is proportional to the volumetric flux across the face, which enables us to consider the streamlines as carrying approximately equal amounts of fluids, i.e., $q_{sl} \approx C$ for some constant C. An advantage of this approach is that the sums in (8) and (9) can be computed incrementally as streamlines are traced (Batycky, 1997) without knowing the associated volumetric flux, thus allowing completely independent processing of streamlines.

For the volumetric mapping (8) to make sense, each grid-block should in principle be traversed by at least one streamline. In general, there will be a number of grid-blocks that are not traversed by any of the streamlines

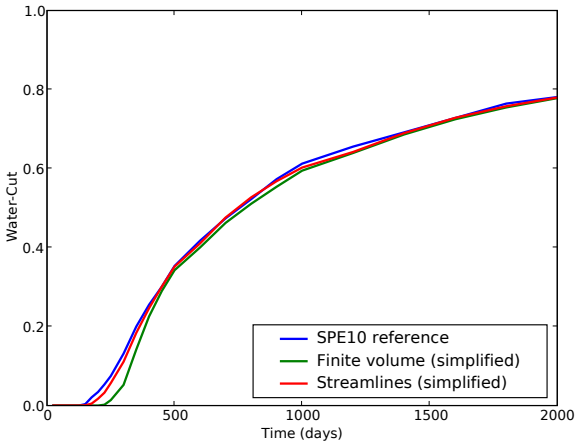

Fig. 1— Water-cuts for Producer 1 computed by a commercial streamline simulator on the original SPE10 model, along with our finite-volume and streamline solutions for the simplified problem (no compressibility and gravity).

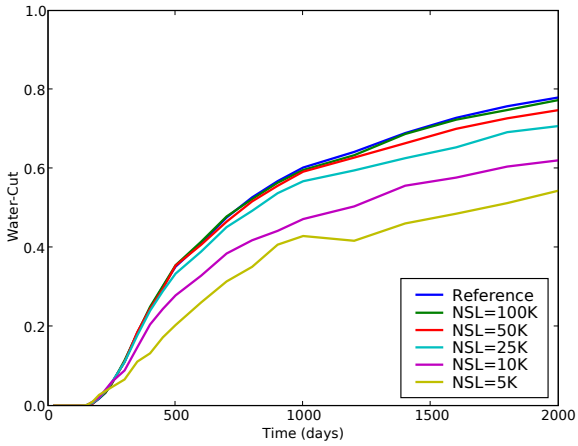

Fig. 2— Water-cuts for Producer 1 for various number of streamlines. (In the legend, 1K = 1 000.)

traced from the faces of injector-blocks. To make the streamlines cover all grid blocks, one can perform an additional tracing process where one picks a point inside one of the untraced blocks and traces a streamline from this point forward to a producer and backward to an injector, or one can follow Batycky (1997) and only trace streamlines back to a block which is already traversed by streamlines. The process is continued until there are no untraced blocks. Alternatively, one may simply ignore the untraced blocks, as these often are in regions that have a very small contribution to the production characteristics. To keep the amount of streamline tracing at a minimum we here employ the latter approach.

Mass-Balance Problems

For the particular streamline implementation described above, the overall accuracy will primarily depend on the number of streamlines used in the simulation. To illustrate the typical behaviour as the number of streamlines is reduced, we consider Model 2 from the 10$^{\text{th}}$ SPE Comparative Solution Project (Christie and Blunt, 2001), which is a large 3-D reservoir model consisting of $60 \times 220 \times 85$ grid-blocks, each of size 20ft $\times$ 10ft $\times$ 2ft. The model is a geostatistical realisation of a Brent sequence. The top 35 layers represent the Tarbert formation, which is a prograding near-shore environment. The lower 50 layers represent the Upper Ness formation, which is fluvial.

The model is produced using a five-spot pattern of vertical wells, where the central injector has an injection rate of 5 000 bbl/day (reservoir conditions), and the producers in each of the four corners of the model produce at 4 000 psi bottom hole pressure. As in the original model, we use quadratic relative permeability curves with $S_{\text{wc}} = S_{\text{or}} = 0.2$. The initial saturation is $S_0 \equiv S_{\text{wc}}$, and oil and water viscosities are $\mu_o = 3.0$ cP and $\mu_w = 0.3$ cP, respectively. For simplicity, we have neglected gravity and compressibility, since these have smaller impact on the production curves than the numerical diffusion inherent in any numerical scheme. This can be seen in **Fig. 1**, which compares a fine-grid reference solution from the SPE10 website (`http://www.spe.org/csp/`) with two fine-grid solutions for the simplified physical model; one computed by a first-order upstream finite-volume method, and the other computed by the "standard" streamline method introduced above with 600 000 streamlines. The simplified streamline solution will therefore be used as a reference solution in the rest of the paper. We note that we use the same time-steps as the reference solver: 25 steps with smaller step-sizes in the beginning of the simulation.

Figure 2 displays the water-cut in Producer 1 for simulations with various number of streamlines. The figure shows that the water production is underestimated when the number of streamlines is too small. Since the correct total amount of injected water is distributed among streamlines at the injecting end of each streamline, there must effectively be a loss of mass in the method. We can quantify this loss by, e.g., computing the relative mass-balance error for water in each time-step,

$$\epsilon_{\Delta t} = \frac{\text{INJ}_{\Delta t} - \text{PRD}_{\Delta t} + \text{FIP}_t - \text{FIP}_{t+\Delta t}}{\text{INJ}_{\Delta t}}, \qquad (10)$$

which is equivalent to the volume-balance error, since we have assumed incompressibility. **Figure 3** shows that the errors increase rapidly in the beginning of the simulation and decay slowly as the corresponding water-cut curves increase.

Spatial Errors in Streamline Discretizations. To explain the origin of the observed mass-balance errors we follow Jimenez et al. (2005): Using the bi-streamfunctions (Bear, 1972) for which,

$$\mathbf{u} = \nabla\psi \times \nabla\chi, \qquad (11)$$

we can define an alternative curvlinear coordinate system $(\tau,\ \phi,\ \chi)$ for three-dimensional space where the velocity $\mathbf{u}$, and hence the τ coordinate curves, i.e., the streamlines, will be orthogonal to the ψ and χ coordinate curves. It is this orthogonality relation (11) that is responsible for

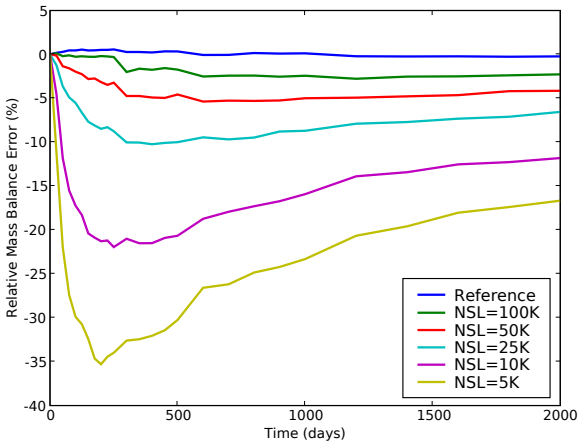

Fig. 3— Relative mass-balance errors in the streamline method for various number of streamlines.

the particularly simple form of the saturation equation (5) along streamlines. The discretization along streamlines is defined by the streamline grids obtained from the tracing algorithm, while the transversal discretization is determined by the partition of the volume into streamtubes, or in our case, the distribution of streamlines and the association of fluxes to streamlines.

The pore volume of this discretization will generally not match the pore volume of the original grid, which will lead to mass-balance errors when mapping saturation between the streamlines and the pressure grid. From (7) we have that the streamline pore volume is given by,

$$\mathrm{V}_{sl} = \sum_{sl} q_{sl}\tau_{sl}, \tag{12}$$

but both q_{sl} and τ_{sl} are subject to approximation errors. As noted by Matringe and Gerritsen (2004), the simple semi-analytical streamline tracing approach gives errors, even if given analytical fluxes on the grid-block faces of Cartesian grids, since the velocity field is approximated by a piecewise bilinear function. Assigning equal fluxes to all streamlines is also slightly inaccurate since the fluxes actually represent the velocity integral across the cross-section of the associated streamtube. Even if the velocity is considered to be constant on injector-block faces, errors are introduced because the initial cross-section areas of the streamtubes will not be equal unless the number of starting points on each face is a perfect square. However, as the number of streamlines is reduced, the primary source of errors may be the assumption that the time-of-flight along a streamline is a good approximation to the average time-of-flight over cross-sections of the associated streamtube. To illustrate, **Fig. 4** shows the time-of-flight values for numerous points on the cross-section of two grid-blocks from the fluvial formation of the SPE10 model discussed above. Here, the variation in τ is actually of the same magnitude as the values themselves, hence the aforementioned assumption may yield very inaccurate streamline volumes.

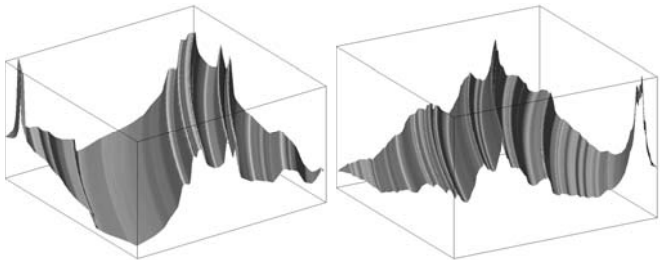

Fig. 4— Time-of-flight in two different grid blocks of Layer 76 in the SPE10 model sampled in 200×200 evenly distributed points inside each block.

Improving the Mass Balance

The presence of mass-balance errors in the streamline solutions is a well-known problem, and improving the accuracy and mass-balance properties of streamline methods is an active area of research. However, much of this research seems to be geared toward problems with complicated geometry and/or complicated physics. For instance, streamline tracing on corner-point geometry has been investigated by Jimenez et al. (2005) and Hægland et al. (2006), while Gerritsen et al. (2005; and related works) studied issues such as streamline distribution and more accurate mapping algorithms in the context of gas injection simulations. The latter works represent a fundamental change of the standard streamline approach, where streamlines are no longer viewed as fluid carriers, and saturations are mapped to the underlying grid using a statistical regression technique (kriging). This gives a large degree of freedom in distributing streamlines in the reservoir, but involves the solution of linear systems for the kriging weights, which may dominate the computation time for problems such as water-flooding, where the computation of the one-dimensional solutions is extremely efficient. Also, the natural way of estimating well production (9) is no longer applicable unless a volumetric flux is associated with each streamline.

Within the framework of regarding streamlines as fluid carriers, (12) shows that there are really only two parameters we can play with to improve the mass-balance properties of streamline methods, namely the streamline fluxes, q_{sl}, and the streamline time-of-flights, τ_{sl}. The exact properties of these are functions of the particular choices made in the streamline method implementation, and as noted in the previous section, both parameters may contain large errors for the specific implementation considered here. The close match between the reference streamline simulation and the finite-volume solver (**Fig. 1**) implies that the streamline tracing is sufficiently accurate for this problem, although we note that more accurate tracing on Cartesian grids is possible, for instance by utilizing velocity fields computed with higher-order mixed finite-element methods (Matringe et al., 2006).

The association of fluxes with streamlines is within the present framework related to the distribution of streamlines, since we assume equal flux for all streamlines. To bring the streamline fluxes closer to the actual velocity integral over the streamtube cross-section, we may consider scaling q_{sl} according to the interpolated velocity at the starting point and the cross-section area of the associated

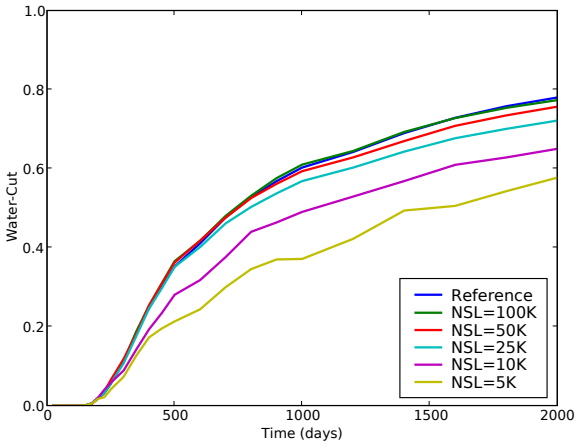

Fig. 5— Producer 1 water-cut for various number of streamlines when starting streamlines from both injectors and producers, and scaling the streamline fluxes according to the perpendicular bisection areas.

streamtube (Ponting, 1998; Pallister and Ponting, 2000). Lifting the restriction of equal streamline fluxes also makes it possible to apply other streamline distribution schemes. For instance, in situations where there is a large variation in total fluid rates between different producers, it may be beneficial to start streamlines also on the faces of well-blocks containing producers to ensure that sufficient accuracy is achieved even for wells with small rates.

To study the influence of these factors, we perform simulations where the starting points of streamlines are generated on the block-faces of both injectors and producers. For each face of grid-blocks containing an injector, the total volumetric flux is divided among the streamlines penetrating the face, with weights given by the areas of a perpendicular bisection of the block face. We have chosen to ignore the velocity variation over the faces since Ponting (1998) found that this only had a minor effect. **Figure 5** shows that this alternative approach to streamline distribution and flux computation is not significantly better than the original approach for the SPE10 case, although a slight improvement is detectable.

The results above indicate that the primary source of error, as the number of streamlines is reduced, is indeed that the time-of-flight along streamlines is not an accurate representation of the average time-of-flight over cross-sections of the associated streamtubes. Increasing the number of streamlines decreases the streamtube cross-sections and hence reduces these errors. However, considering the very large time-of-flight variation shown in **Fig. 4**, it appears that a large number of streamlines is necessary to obtain accurate streamline volumes and thereby low mass-balance errors. On the other hand, if we insist on keeping the number of streamlines low, we can use the fact that mass should be conserved, and correct the computed time-of-flight values to enforce the mass-balance constraint. We will have exact conservation of mass if the streamline volume matches the true pore volume, i.e., $\sum_{sl} V_{sl,i} = V_i$, in every grid-block touched by streamlines. In this case the mappings between streamlines and the pressure grid preserve mass. Indeed, for the grid-to-streamline mapping (6) we have,

$$\begin{aligned} V_{w,grid} = \sum_i V_i S_i &= \sum_i \Big(\sum_{sl} V_{sl,i} \Big) S_i \\ &= \sum_{sl} \sum_i V_{sl,i} S_{sl,i} = V_{w,sl}, \end{aligned} \tag{13}$$

and similarly for the streamline-to-grid mapping (8),

$$\begin{aligned} V_{w,sl} = \sum_{sl} \sum_i V_{sl,i} S_{sl,i} &= \sum_i \sum_{sl} \frac{V_i}{\sum_{sl} V_{sl,i}} V_{sl,i} S_{sl,i} \\ &= \sum_i V_i S_i = V_{w,grid}, \end{aligned} \tag{14}$$

where $V_{w,grid}$ and $V_{w,sl}$ are the total volumes of water on the the pressure and streamline grids, respectively. Since the streamline flux is constant along the streamline path, our only option for ensuring $\sum_{sl} V_{sl,i} = V_i$ is to modify the local time-of-flight values, $\Delta\tau_{sl,i}$. Specifically, prior to solving the one-dimensional saturation equation (5) along streamlines, we propose to scale the time-of-flight values in block i by a factor $\alpha_i = V_i / \sum_{sl} V_{sl,i}$. This means that streamlines can no longer be processed independently of each other, and we need to store streamlines in memory, or alternatively perform the complete tracing procedure twice; once to compute the values of α_i, and then a second time for the solution of the one-dimensional problems. The memory requirement for storing streamlines is usually lower than what is necessary for the solution of the pressure equation (1), hence the former approach is preferable since tracing is an expensive process.

Scaling the time-of-flight values amounts to locally stretching or shrinking the grid on which the one-dimensional saturation equation (5) is solved. Unless the errors in the streamline tracing are large, the grid obtained by the tracing is the correct one, and the modifications will result in less accurate one-dimensional solutions. In other words, by choosing to enforce mass conservation, we locally introduce errors, but as we demonstrate below, the global properties of the resulting solutions are better. However, we must take special care not to ruin important characteristics of the correct one-dimensional solutions. A quantity of particular interest is the breakthrough-time for producers, and to make sure this is estimated correctly, we only apply the time-of-flight scaling along streamlines where breakthrough has occurred.

Figures 6 and **7** show water-cuts for Producer 1 and and relative mass-balance errors for various number of streamlines when using the modified streamline approach. Mass-balance errors are still large initially since the time-of-flight scaling is only applied after breakthrough, but the errors decrease rapidly. The improvement on the water-cut curves is significant, to say the least, with as few as 5 000 streamlines giving acceptable results. We can quantify the error in a water-cut curve $w(t)$ by,

$$\delta(w) = \|w - w^{\mathrm{ref}}\|_2 / \|w^{\mathrm{ref}}\|_2, \tag{15}$$

and **Table 1** shows that the results are similar also for the other three producers. For completeness, **Table 1** also

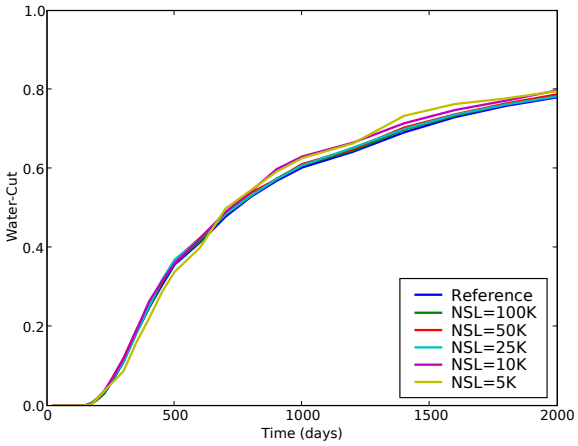

Fig. 6— Water-cuts for Producer 1 for various number of streamlines when using the modified streamline method.

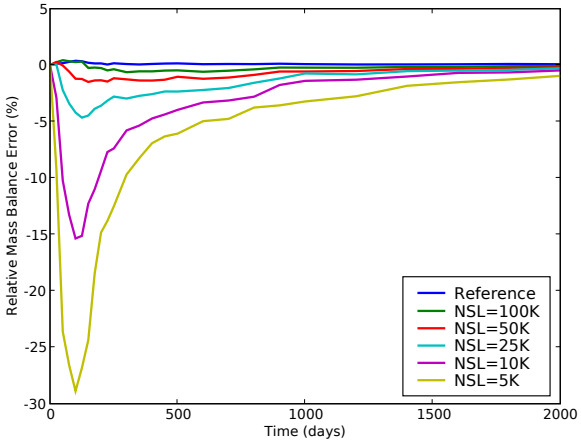

Fig. 7— Relative mass-balance errors in the streamline method for various number of streamlines when using the modified streamline method.

shows the corresponding results for the standard streamline approach, where we have started streamlines in both injectors and producers and used the perpendicular bisection approach above to assign fluxes to streamlines, as we previously showed that this gives slightly better results.

Since the time-of-flight scaling introduces local errors in the one-dimensional saturation solutions, we may ask if the global saturation solutions now are less accurate than for the original approach. We therefore compute saturation errors in the porosity-weighted L^1-norm,

$$\delta(S) = \|\phi(S - S^{\text{ref}})\|_1 / \|\phi S^{\text{ref}}\|_1, \qquad (16)$$

for each time-step, and the average through the simulation is displayed in **Table 1**. The results show that the modified streamline method gives slightly more accurate saturation fields than the original method for the same number of streamlines, but generally does not allow a significant reduction in the number of streamlines if one is to retain a certain accuracy.

If one, on the other hand, is mainly interested in accurate production curves, **Table 1** shows that the number of streamlines can be significantly reduced. For instance, if we allow a 5% water-cut error as measured by (15), we see that we may need 50 000 streamlines in the original approach, whereas 5 000 streamlines is sufficient when using the modified method. This yields a significant speedup for the transport part of the simulation, since the computation time associated with transport in theory scales linearly with the number of streamlines. The timing results in **Table 1** show that the actual scaling is not truly linear as the number of streamlines becomes very small. However, this is to be expected since our simulator is optimized for relatively large numbers of streamlines and otherwise negligible overhead associated with streamline distribution, flux computations, and saturation mappings may become significant when using a small number of streamlines. Still, we see that going from 5 000 to 50 000 streamlines gives at least five times speedup for the transport step. Finally, we note that as the number of streamlines is reduced, the total simulation time is dominated by the solution of the pressure equation (1). To obtain a more substantial speedup for the overall simulation, the modified streamline method should be considered in combination with approximate pressure solution techniques, e.g., with a multiscale method as discussed by Aarnes et al. (2005).

A Simpler Example

Since our proposed modification to the streamline method introduces local errors along streamlines, we might suspect that the approach only represents an improvement for difficult models where the original streamline method gives very large errors, and that it might yield significantly less accurate results for simpler models. In this section we therefore apply the modified and original streamline methods to a small model with homogeneous permeability and porosity data. In particular, we use a $32 \times 32 \times 8$ model with grid-block aspect ratio $1 : 1 : 0.1$, with wells placed in a five-spot pattern and the four producers producing at equal bottom-hole pressures. We assume quadratic relative permeability curves with zero residual oil and water saturations, and perform simulations for three different values of the end-point mobility ratio $M_{\text{end}} = \mu_o/\mu_w$, corresponding to unit mobility ratio ($M_{\text{end}} = 1$), favourable displacement ($M_{\text{end}} = 0.1$) and high-mobility ratio displacement ($M_{\text{end}} = 10$), respectively. The dimensionless simulation time was 2.0 PVI, and for all three scenarios we verified that the chosen number of time-steps was sufficient for stability of the sequential time-stepping scheme.

Tables 2 – 4 show the water-cut errors for both streamline approaches with various number of streamlines in each of the three scenarios. The results are indecisive and we cannot conclude that the modified streamline method significantly improves the accuracy of the production curves for this homogeneous model. On the other hand, the time-of-flight scaling does generally not cause the new approach to perform worse than the original method, either. This implies that the modified streamline approach can be safely applied also for simple datasets.

Adaptive Streamline Coverage The results in **Tables 2 – 4** also show that there is a large accuracy difference, for both methods, between the three displacement scenarios. In particular, **Table 3** shows that a larger number of streamlines is required to obtain accurate results for favourable displacement conditions. The large errors observed when using few streamlines for this piston-like displacement are caused by insufficient streamline coverage, since we do not ensure that all grid-blocks are traversed by streamlines. This leads to errors in the computed pressure and velocity fields, thus shifting the predicted time of breakthrough. For scenarios with high mobility-ratios, the pressure/velocity solutions are less sensitive to errors in the underlying saturation field, because the saturation variation is generally much smoother.

To alleviate the accuracy problems for favourable displacement conditions, we could trace streamlines through every grid-block, using, e.g., the approach of Batycky (1997). However, many grid-blocks will typically be located in low-flow regions that do not significantly affect the solution. We therefore propose an adaptive approach to streamline coverage, where we only demand that a given fraction β of the pore volume should be traversed by streamlines. Before the tracing starts, grid-blocks are sorted in descending order by absolute velocity $|\mathbf{u}|$, and we trace back from untouched blocks in sorted order until the given pore-volume target has been met. We also ensure that each well is properly covered by starting a specified number of streamlines from each well, with the distribution of streamlines on well-block faces given according to the fluxes, as before.

In **Tables 5 – 7** we have displayed the average number of streamlines and water-cut errors when applying this adaptive approach in combination with the modified streamline method for the three different displacement scenarios. Initially we trace 100 streamlines from each well, which is why the minimum number of streamlines is 500. Compared with **Tables 2 – 4** we see that tracing streamlines adaptively based on flow velocity gives more accurate results using fewer streamlines. As expected, the optimal value of β depends on the displacement conditions, with piston-like displacement requiring a larger fraction of the pore volume to be covered. On the other hand, the adaptivity has barely a significant effect for the scenario with high-mobility ratio, where we actually could have used even fewer streamlines. This helps explain why we obtained accurate results using extremely few streamlines for the SPE10 model above.

Application Example: History Matching

The results and discussion above clearly indicate that the modified streamline method is most suitable for applications where one is primarily interested in accurate production responses rather than accurate predictions of the dynamic distribution of fluids. Examples of such applications are history matching and ranking of multiple equiprobable geostatistical models.

In the following we consider history-matching of a high-resolution geomodel using a generalized travel-time inversion method (Vasco et al., 1999; He et al., 2002). The inversion method consists of four major steps that are repeated until a satisfactory match in production data is obtained: (i) Multiscale-streamline simulation to compute production responses at the wells. (ii) Quantification of the mismatch between observed and computed production responses via a generalized travel time, and computation of an optimal time shift that systematically shifts the computed production responses towards the observed data. (iii) Computation of streamline-based analytic sensitivities of water-cut data with respect to permeability. (iv) Updating of grid-block permeability values to match the production history via inverse modelling (minimization of a misfit functional). More details of the inversion procedure are given in (Stenerud et al., 2007).

We consider a synthetic geomodel given by a uniform Cartesian grid with $256 \times 128 \times 32$ cells, where each cell has dimensions 10m×10m×2m. A total number of 32 vertical injectors and 69 vertical producers are included in the simulation model. The injectors inject water at a constant total volumetric reservoir rate of 1609 bbl/day, and each producer produces fluids at a constant reservoir volume rate fulfilling the total voidage rate. The flow model assumes quadratic relative permeability curves with an endpoint mobility ratio of $M_{\text{end}} = 5$.

The production history to be matched consists of 2475 days of water-cut data from the 69 producers, obtained by simulation on a reference geomodel having log-normally distributed permeability with mean 2.2 mD and values in the interval [0.017,79.5] mD; see **Fig. 8**. An initial permeability model was generated by assuming the permeability to be known in each well block and using sequential Gaussian simulation to generate multiple realizations.

The inversion algorithm converged in six iterations, after which the misfit in time-shift and amplitude (see Stenerud et al., 2007) were reduced to 7.8% and 53.6% of their initial values, respectively. In the inversion, we use the original streamline method with 500 000 streamlines and 15 uniform pressure steps of 165 days for each forward simulation. To solve the pressure equation we use an approximate, but highly efficient multiscale method (Aarnes and Lie, 2004). The total time for the whole inversion was 1 hour and 27 minutes on a Linux workstation with a 2.4 GHz Intel Core 2 Duo processor with 4Mb cache and 3 Gb memory. Using the modified streamline method we were able to reduce the number of streamlines to 50 000, and thereby reduce the total time for inversion to 39 minutes without reducing significantly the quality of the obtained history match. In fact, the time-shift and amplitude residuals were reduced to 7.6% and 48.7% of their original values, respectively.

Concluding Remarks

In this paper we have introduced a modified streamline method which greatly reduces the mass-balance errors when simulating large and complex reservoir models using few streamlines. Improved mass-conservation properties are achieved by locally scaling the time-of-flight grids, on which the one-dimensional transport equations are solved, to enforce mass conservation in the mappings between the Eulerian pressure grid and the Lagrangian streamlines. As a consequence, we are able to obtain accurate production curves on a million grid-block reservoir model with five

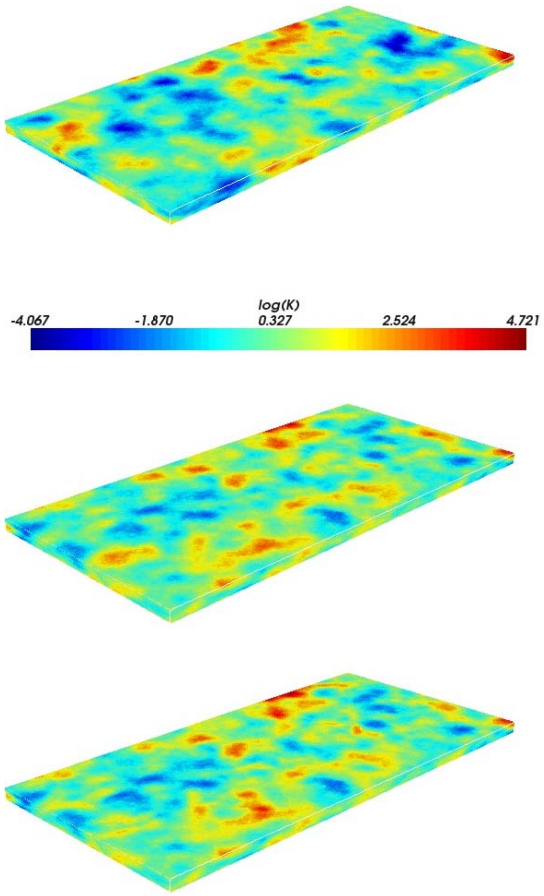

Fig. 8— Geomodels for the 3D history-matching case: reference model (top) initial model (middle), and final match (bottom).

wells using only 5 000 streamlines, and the total simulation time is less than ten minutes using a standard desktop computer.

We verified that the modified approach is applicable also to simple models by showing that its performance was similar to that of the original method on a homogeneous dataset. We also demonstrated that favourable, piston-like displacement might be challenging to simulate using few streamlines, and proposed an adaptive approach to streamline coverage based on tracing streamlines from untouched cells in high-flow regions until a given fraction of the pore volume has been traversed.

We have not considered improvements in the algorithms for mapping saturations between streamlines and the pressure grid, and the modified approach does therefore not give significantly better saturation solutions than the original method. This implies that the modified streamline method is best suited for applications that depend heavily on rapid estimation of production responses. As an example we demonstrated significant speed-up for a history-match of a million grid-block model with 32 injectors and 69 producers.

Finally, we remark that our modified method probably has an even larger potential for non-Cartesian grids, where Pollock's method for analytical tracing of streamlines introduces large errors, both in the time-of-flights and in the actual streamline paths; see Hægland et al. (2006) for further details.

Nomenclature

Roman letters

A	Area
C	Constant
f	Fractional flow
FIP	Volume of fluid (water) in place
$\mathbf{K}$	Permeability tensor
INJ	Injected volume (water)
k_r	Relative permeability
M_{end}	End-point mobility ratio
p	Pressure
PRD	Produced volume (water)
s	Distance along streamline
S	Saturation
S_{wc}	Connate water saturation
S_{or}	Residual oil saturation
t	Time
$\mathbf{u}$	Total Darcy velocity
V	Volume
w	Water-cut curve
q	Volumetric rate

Greek letters

$\delta(\cdot)$	Relative error
ϵ	Relative mass balance error
λ	Mobility
μ	Viscosity
ϕ	Porosity
ψ,χ	Bi-streamfunctions
τ	Time-of-flight
ζ	Space coordinate along streamline

Subscripts

i	Block number
j	Phase number
sl	Streamline number
st	Streamtube number
o, w	Oil and water phases
t, tot	Total
Δt	Time-step

Acknowledgements

The authors are grateful to V. R. Stenerud for providing the history-matching example, and to J. R. Natvig for providing the plot of time-of-flight within a grid cell. The authors gratefully acknowledge financial support from the Research Council of Norway; Kippe and Lie under grants number 152732/S30 and 158908/I30, and Hægland under grant number 173875/I30.

References

J. E. Aarnes and K.-A. Lie. Toward reservoir simulation on geological grid models. In *Proceedings of the 9th European Conference on the Mathematics of Oil Recovery*, Cannes, France, 2004. EAGE.

J. E. Aarnes, V. Kippe, and K.-A. Lie. Mixed multiscale finite elements and streamline methods for reservoir simulation of large geomodels. *Adv. Water Resour.*, 28(3):257–271, 2005.

R.P. Batycky. *A Three-Dimensional Two-Phase Field-Scale Streamline Simulator*. PhD thesis, Stanford University, Dept. of Petroleum Engineering, 1997.

J. Bear. *Dynamics of Fluids in Porous Media*. American Elsevier, New York, 1972.

F. Bradtvedt, K. Bratvedt, C.F. Buchholz, T. Gimse, H. Holden, L. Holden, R. Olufsen, and N.H. Risebro. Three-dimensional reservoir simulation based on front tracking. *North Sea Oil and Gas Reservoirs*, III:247–257, 1994.

F. Bratvedt, K. Bratvedt, C.F. Buchholz, T. Gimse, H. Holden, L. Holden, and N.H. Risebro. Frontline and frontsim: two full-scale, two-phase, black oil reservoir simulators based on front tracking. *Surv. Math. Ind.*, (3):185–215, 1993.

M.A. Christie and M.J. Blunt. Tenth SPE comparative solution project: A comparison of upscaling techniques. *SPE Reservoir Eval. Eng.*, 4(4):308–317, 2001. url: www.spe.org/csp.

M. Crane, F. Bratvedt, K. Bratvedt, P. Childs, and R. Olufsen. A fully compositional streamline simulator. In *SPE Annual Technical Conference and Exhibition, Dallas, TX, October 1 - 4, 2000*, SPE 63156, 2000.

A. Datta-Gupta and M. J. King. *Streamline Simulation: Theory and Practice*. SPE Textbook Series. to appear.

G. Di Donato and M.J. Blunt. Streamline-based dual-porosity simulation of reactive transport and flow in fractured reservoirs. *Water Resour. Res.*, 40(W04203), 2004. doi:10.1029/2003WR002772.

M.G. Gerritsen, K. Jessen, B.T. Mallison, and J. Lambers. A fully adaptive streamline framework for the challenging simulation of gas-injection processes. In *SPE Annual Technical Conference and Exhibition, Houston, TX, October 9 - 12, 2005*, SPE 97270, 2005.

H. Hægland, H.K. Dahle, G.T. Eigestad, K.-A. Lie, and I. Aavatsmark. Improved streamlines and time-of-flight for streamline simulation on irregular grids. *Advances in Water Resources*, 2006. doi:10.1016/j.advwatres.2006.09.002.

Z. He, A. Datta-Gupta, and S. Yoon. Streamline-based productoin data integration with gravity and changing field conditions. *SPE J.*, 7(4):423–436, 2002.

H. Holden and N.H. Risebro. *Front Tracking for Hyperbolic Conservation Laws*, volume 152 of *Applied Mathematical Sciences*. Springer, New York, 2002.

E. Jimenez, K. Sabir, A. Datta-Gupta, and M.J. King. Spatial error and convergence in streamline simulation. In *SPE Reservoir Simulation Symposium, Houston, TX, January 31-February 2, 2005*, SPE 92873, 2005.

M. J. King and A. Datta-Gupta. Streamline simulation: A current perspective. *In Situ*, 22(1):91–140, 1998.

S.F. Matringe and M.G. Gerritsen. On accurate tracing of streamlines. In *SPE Annual Technical Conference and Exhibition, Houston, TX, September 26 - 29, 2004*, SPE 89920, 2004.

S.F. Matringe, R. Juanes, and H.A. Tchelepi. Robust streamline tracing for the simulation of porous media flow on general triangular and quadrilateral grids. *JCP*, 2006. doi:10.1016/j.jcp.2006.07.004.

I.C. Pallister and D.K. Ponting. Asset optimization using multiple realizations and streamline simulation. In *SPE Asia Pacific Conference on Integrated Modelling for Asset Management, Yokohama, Japan, 25 - 26 April 2000*, SPE 59460, 2000.

D.W. Pollock. Semi-analytical computation of path lines for finite-difference models. *Ground Water*, 26(6):743–750, 1988.

D.K. Ponting. Hybrid streamline methods. In *SPE Asia Pacific Conference on Integrated Modelling for Asset Management, Kuala Lumpur, Malaysia, 23 - 24 March 1998*, SPE 39756, 1998.

V.R. Stenerud, V. Kippe, A. Datta-Gupta, and K.-A. Lie. Adaptive multiscale streamline simulation and inversion for high-resolution geomodels. In *SPE Reservoir Simulation Symposium, Houston, TX, February 26–28, 2007*, SPE 106228, 2007.

K. Stüben. *Algebraic Multigrid (AMG): An Introduction with Applications*. Academinc Press, 2000. Guest appendix in the book *Multigrid* by U. Trottenberg and C.W. Oosterlee and A. Schüller.

M.R. Thiele. Streamline simulation. In *8th International Forum on Reservoir Simulation*, Stresa / Lago Maggiore, Italy, 20-24 June 2005.

M.R. Thiele, R.P. Batycky, and M.J. Blunt. A streamline-based field-scale compositional reservoir simulator. In *SPE Annual Technical Conference and Exhibition, San Antonio, TX, October 5 - 8, 1997*, SPE 38889, 1997.

D.W. Vasco, S. Yoon, and A. Datta-Gupta. Integrating dynamic data into high-resolution models using streamline-based analytic sensitivity coefficients. *SPE J.*, pages 389–399, 1999.

NSL	O/M	P1	P2	P3	P4
2000	O	5.07e-02	2.33e-02	3.11e-02	2.90e-02
	M	3.93e-02	2.52e-02	2.69e-02	2.89e-02
1750	O	4.31e-02	2.86e-02	3.30e-02	2.86e-02
	M	3.64e-02	2.18e-02	2.37e-02	2.23e-02
1500	O	5.08e-02	2.91e-02	4.59e-02	3.21e-02
	M	5.11e-02	3.92e-02	3.15e-02	3.82e-02
1250	O	6.66e-02	5.21e-02	6.25e-02	5.49e-02
	M	6.30e-02	3.51e-02	4.55e-02	3.92e-02
1000	O	5.56e-02	4.33e-02	5.78e-02	3.97e-02
	M	4.73e-02	3.76e-02	5.00e-02	4.09e-02
750	O	9.25e-02	8.73e-02	9.09e-02	9.17e-02
	M	7.37e-02	7.03e-02	5.47e-02	7.30e-02
500	O	1.44e-01	1.12e-01	1.06e-01	1.15e-01
	M	1.19e-01	9.82e-02	9.64e-02	1.10e-01
250	O	1.68e-01	2.15e-01	2.43e-01	2.19e-01
	M	1.49e-01	1.61e-01	1.77e-01	1.59e-01

Table 2— Water-cut errors, $\delta(w)$, on the homogeneous model for the original (O) and modified (M) versions of the streamline method, when the end-point mobility ratio $M_{\text{end}} = 1$.

NSL	Method	P1	P2	P3	P4	$\delta(S)$	T_{sl} (s)	T_{tot} (s)
100 000	Original	8.91e-03	6.24e-03	2.44e-03	2.99e-03	2.75e-02	508.92	974.94
	Modified	9.86e-03	4.61e-03	1.97e-03	3.67e-03	2.83e-02	508.20	979.03
50 000	Original	2.53e-02	1.72e-02	6.42e-03	9.38e-03	4.00e-02	266.48	728.42
	Modified	1.66e-02	7.88e-03	3.72e-03	7.03e-03	3.81e-02	265.87	727.79
25 000	Original	6.49e-02	4.85e-02	1.74e-02	2.28e-02	5.89e-02	147.36	608.46
	Modified	1.43e-02	1.47e-02	8.12e-03	7.12e-03	5.27e-02	146.23	613.00
10 000	Original	1.78e-01	1.29e-01	5.53e-02	7.30e-02	9.54e-02	75.65	541.17
	Modified	3.26e-02	1.94e-02	1.56e-02	1.38e-02	8.06e-02	75.33	545.09
5 000	Original	3.20e-01	2.30e-01	1.02e-01	1.30e-01	1.29e-01	50.91	512.75
	Modified	4.25e-02	2.19e-02	1.86e-02	2.37e-02	1.12e-01	51.74	516.63

Table 1— Errors in water-cuts $\delta(w)$ for producers P1 to P4, saturation error $\delta(S)$, computational time for the streamline part of the simulation T_{sl}, and total computation time T_{tot} for the original and modified streamline methods on the SPE10 model for various number of streamlines (NSL).

NSL	O/M	P1	P2	P3	P4
2000	O	4.56e-02	9.18e-02	8.97e-02	9.46e-02
	M	4.43e-02	9.30e-02	8.97e-02	9.47e-02
1750	O	3.29e-02	6.53e-02	6.78e-02	5.17e-02
	M	3.07e-02	6.44e-02	7.09e-02	5.08e-02
1500	O	7.01e-02	1.20e-01	8.98e-02	1.05e-01
	M	5.27e-02	1.13e-01	8.96e-02	1.04e-01
1250	O	6.76e-02	1.13e-01	1.42e-01	8.19e-02
	M	4.60e-02	1.09e-01	1.42e-01	6.32e-02
1000	O	1.40e-01	1.62e-01	1.76e-01	1.67e-01
	M	1.39e-01	1.62e-01	1.76e-01	1.67e-01
750	O	3.40e-01	3.14e-01	3.39e-01	3.57e-01
	M	3.39e-01	3.15e-01	3.40e-01	3.57e-01
500	O	4.26e-01	4.50e-01	4.65e-01	4.69e-01
	M	4.25e-01	4.34e-01	4.64e-01	4.61e-01
250	O	7.79e-01	8.20e-01	8.44e-01	7.99e-01
	M	7.86e-01	8.17e-01	8.42e-01	8.00e-01

Table 3— Water-cut errors, $\delta(w)$, on the homogeneous model for the original (O) and modified (M) versions of the streamline method, when the end-point mobility ratio $M_{\text{end}} = 0.1$.

NSL	O/M	P1	P2	P3	P4
2000	O	2.55e-02	1.33e-02	5.36e-02	1.35e-02
	M	2.58e-02	2.45e-02	2.33e-02	8.44e-03
1750	O	2.89e-02	1.36e-02	6.15e-02	1.04e-02
	M	2.78e-02	1.94e-02	2.63e-02	8.13e-03
1500	O	3.37e-02	1.79e-02	4.43e-02	1.92e-02
	M	3.14e-02	1.00e-02	3.88e-02	9.23e-03
1250	O	3.93e-02	2.42e-02	4.93e-02	2.60e-02
	M	2.63e-02	2.61e-02	5.36e-02	2.72e-02
1000	O	5.33e-02	6.55e-02	3.33e-02	3.19e-02
	M	6.68e-02	2.29e-02	5.79e-02	4.14e-02
750	O	5.05e-02	3.52e-02	4.68e-02	4.27e-02
	M	5.84e-02	2.73e-02	5.09e-02	4.79e-02
500	O	6.97e-02	3.53e-02	5.19e-02	4.42e-02
	M	3.49e-02	4.35e-02	5.22e-02	3.14e-02
250	O	7.07e-02	9.37e-02	1.04e-01	1.01e-01
	M	7.42e-02	9.58e-02	1.20e-01	8.96e-02

Table 4— Water-cut errors, $\delta(w)$, on the homogeneous model for the original (O) and modified (M) versions of the streamline method, when the end-point mobility ratio $M_{\text{end}} = 10$.

β	NSL	P1	P2	P3	P4
1.0	875	3.54e-02	3.08e-02	2.50e-02	3.92e-02
0.9	714	3.86e-02	3.35e-02	3.14e-02	3.89e-02
0.8	576	4.74e-02	3.11e-02	2.28e-02	3.07e-02
0.7	500	6.88e-02	5.88e-02	7.22e-02	4.83e-02
0.6	500	6.83e-02	6.37e-02	7.03e-02	5.09e-02

Table 5— Average number of streamlines and water-cut errors, $\delta(w)$, on the homogeneous model for various values of β, when the end-point mobility ratio $M_{\text{end}} = 1$.

β	NSL	P1	P2	P3	P4
1.0	873	1.17e-02	7.52e-03	2.44e-02	1.37e-02
0.9	701	3.28e-02	2.95e-02	4.82e-02	2.17e-02
0.8	560	2.40e-01	2.31e-01	2.72e-01	2.43e-01
0.7	500	3.34e-01	3.85e-01	3.99e-01	3.90e-01
0.6	500	3.60e-01	3.78e-01	3.98e-01	3.86e-01

Table 6— Average number of streamlines and water-cut errors, $\delta(w)$, on the homogeneous model for various values of β, when the end-point mobility ratio $M_{\text{end}} = 0.1$.

β	NSL	P1	P2	P3	P4
1.0	873	3.45e-02	2.21e-02	2.26e-02	2.04e-02
0.9	722	3.42e-02	2.39e-02	2.41e-02	2.79e-02
0.8	616	2.69e-02	2.44e-02	3.35e-02	2.77e-02
0.7	519	2.19e-02	2.50e-02	5.94e-02	2.43e-02
0.6	500	2.39e-02	3.60e-02	6.80e-02	3.49e-02

Table 7— Average number of streamlines and water-cut errors, $\delta(w)$, on the homogeneous model for various values of β, when the end-point mobility ratio $M_{\text{end}} = 10$.